# Three-dimensional fusion computed tomography decreases radiation exposure, procedure time, and contrast use during fenestrated endovascular aortic repair

Michael M. McNally, MD, Salvatore T. Scali, MD, Robert J. Feezor, MD, Daniel Neal, MS, Thomas S. Huber, MD, PhD, and Adam W. Beck, MD, *Gainesville, Fla*

*Objective:* Endovascular surgery has revolutionized the treatment of aortic aneurysms; however, these improvements have come at the cost of increased radiation and contrast exposure, particularly for more complex procedures. Three-dimensional (3D) fusion computed tomography (CT) imaging is a new technology that may facilitate these repairs. The purpose of this analysis was to determine the effect of using intraoperative 3D fusion CT on the performance of fenestrated endovascular aortic repair (FEVAR).

*Methods:* Our institutional database was reviewed to identify patients undergoing branched or FEVAR. Patients treated using 3D fusion CT were compared with patients treated in the immediate 12-month period before implementation of this technology when procedures were performed in a standard hybrid operating room without CT fusion capabilities. Primary end points included patient radiation exposure (cumulated air kerma: mGy), fluoroscopy time (minutes), contrast usage (mL), and procedure time (minutes). Patients were grouped by the number of aortic graft fenestrations revascularized with a stent graft, and operative outcomes were compared.

*Results:* A total of 72 patients (41 before vs 31 after 3D fusion CT implementation) underwent FEVAR from September 2012 through March 2014. For two-vessel fenestrated endografts, there was a significant decrease in radiation exposure (3400 ± 1900 vs 1380 ± 520 mGy; $P = .001$), fluoroscopy time (63 ± 29 vs 41 ± 11 minutes; $P = .02$), and contrast usage (69 ± 16 vs 26 ± 8 mL; $P = .0002$) with intraoperative 3D fusion CT. Similarly, for combined three-vessel and four-vessel FEVAR, significantly decreased radiation exposure (5400 ± 2225 vs 2700 ± 1400 mGy; $P < .0001$), fluoroscopy time (89 ± 36 vs 64 ± 21 minutes; $P = .02$), contrast usage (90 ± 25 vs 39 ± 17 mL; $P < .0001$), and procedure time (330 ± 100 vs 230 ± 50 minutes; $P = .002$) was noted. Estimated blood loss was significantly less ($P < .0001$), and length of stay had a trend ($P = .07$) toward being lower for all patients in the 3D fusion CT group.

*Conclusions:* These results demonstrate that use of intraoperative 3D fusion CT imaging during FEVAR can significantly decrease radiation exposure, procedure time, and contrast usage, which may also decrease the overall physiologic impact of the repair. (J Vasc Surg 2015;61:309-16.)

Fenestrated endovascular aortic repair (FEVAR) is becoming increasingly common and is now commercially available in the United States with recent Food and Drug Administration approval of a customized fenestrated device. With this technological advancement, there is an expected decrease in the physiologic insult to the patient compared with open repair[1-3]; however, this comes with increased radiation and contrast exposure risk during the

procedures.[4] Fluoroscopy is an important radiation source in contemporary practice, and an increasing focus on the effects of cumulative radiation exposure to patients and providers is present in the literature.[4-14] Notably, a recent report demonstrated that FEVAR is one of the most radiation-intensive procedures that vascular specialists perform.[4]

The FEVAR radiation dose is related not only to the fluoroscopy time but also to the density of the abdomen and pelvis and the frequent obliquity that is necessary to visualize target vessels adequately.[13] In addition, these procedures often require large amounts of iodinated contrast, which may be partly responsible for the known decrement in renal function that can occur after FEVAR.[15,16] Importantly, advanced imaging techniques have been shown to decrease operative times and radiation exposure as well as mitigate the need for contrast usage during routine EVAR.[17,18]

Our institution has recently upgraded to a fixed-imaging unit capable of three-dimensional (3D) fusion computed tomography (CT), and we sought to evaluate how this technology has affected the conduct of FEVAR

and whether it has afforded any demonstrable benefit with regard to radiation exposure and contrast usage.

## METHODS

The University of Florida Institutional Review Board (FWA00005790) approved this study protocol (#201300781). A waiver of informed consent was granted because all collected data pre-existed in medical records and no study-related interventions or patient contact occurred. Therefore, the rights and welfare of these patients was not adversely affected.

**Patient selection.** A review of our institutional endovascular aortic database was performed for patients who underwent FEVAR before and after inauguration of a hybrid operating room capable of 3D fusion CT imaging. To mitigate the effect of the learning curve over time, patients treated using 3D fusion CT imaging were compared with patients treated in the immediate 12 months before the availability of the new hybrid unit. Specifically, the dates of collection included patients receiving FEVAR in the 3D fusion CT-capable room beginning in September 2013 vs those treated in the 365 days before.

A single surgeon (A.W.B.) at our institution began offering FEVAR in January 2010. We intentionally excluded the initial 68 cases, of which 48 (69%) were three-vessel or four-vessel fenestration procedures, spanning a 2.5-year period, to minimize the effect of the operative team learning curve on the results of this study. In addition, no significant operative team personnel or device implantation technique changes occurred during the study interval.

The method of target visceral vessel catheterization has been described previously and did not change significantly during the study period.[19] Patients were grouped by the number of fenestrations or branches revascularized (ie, excluding fenestrations or scallops that were not supported with a stent). Patients undergoing a two-vessel FEVAR were compared separately from three-vessel and four-vessel FEVAR patients, and three-vessel and four-vessel patients were grouped to increase numbers for comparison. Demographics, comorbidities, intraoperative characteristics (including adjuncts as defined by the Society for Vascular Surgery standards[20,21]), and postoperative outcomes were abstracted from our prospective database or the electronic medical record, or both, as needed. Comorbidities were defined according to reporting guidelines.[1]

**Clinical practice.** All patients were recovered in a dedicated cardiovascular intensive care unit. Patients were mobilized and given a normal diet on postoperative day 1 if there were no clinical concerns, such as neurologic, cardiopulmonary, gastrointestinal, hematologic, or renal system derangements. Thereafter, patients were transferred to the floor (unless on the spinal drain protocol), and all indwelling lines and catheters were removed if clinical recovery continued to be uneventful. Once patients tolerated a regular diet and received evaluation by physical therapy, they were discharged from the hospital. A restrictive

transfusion protocol exists at our institution, and patients generally receive a transfusion only for a hemoglobin of <7 g/dL unless there is evidence of hypovolemic anemia or cardiac ischemia. The need for spinal drainage was determined by the operating surgeon. Spinal drain protocols did not change during the study interval and have been previously published.[22]

**Equipment and procedural details.** Patients undergoing FEVAR before the 3D-capable operating room (no-CT group) availability were treated in a hybrid operating room using a fixed imaging Infinix VC-i (Toshiba Medical Systems, Tokyo, Japan) ceiling-mounted, single-plane system. Fluoroscopy was generally performed at a low dose of 7.5 frames per second (fps), and digital subtraction angiography (DSA) was performed at 3 fps, unless an increased frame rate was necessary for improved imaging, in which case 6 fps was used. This system was routinely used in conjunction with intravascular ultrasound (IVUS) imaging using a Volcano catheter (Volcano Corp, San Diego, Calif). Before device delivery, IVUS imaging was used to determine branch vessel locations.

After device delivery, a flush catheter was used to perform DSA in the anterior-posterior and lateral projections to mark the branch vessel locations. Next, the device was deployed while the radiopaque fenestration/branch markers were triangulated against the DSA roadmap imaging. DSA imaging was performed intermittently to facilitate vessel catheterization and confirm successful access to the respective target vessels. DSA runs were also routinely used to perform individual completion runs for the branch vessels and a completion aortogram. Contrast was minimized by diluting it to one-third strength (Visipaque 320; GE Healthcare, Hertfordshire, United Kingdom) for hand-injection imaging and to one-half strength for completion imaging.

Use of the 3D fusion CT-capable hybrid operating room began in September 2013, which uses an Artis zee system (Siemens Medical Solutions USA, Inc, Malvern, Pa; http://usa.healthcare.siemens.com/angio/artis-zee/artis-zee). Of note, the radiology technicians for our dedicated vascular operating team underwent advanced imaging training through Siemens before our first procedure, which allowed a rather seamless introduction of this technology into our practice. This unit was also used at a low dose of 7.5 fps, and DSA was performed at 4 fps.

Before the procedure, the operating surgeon used the Leonardo workstation (Siemens AG, Forchheim, Germany) to process the preoperative CT arteriogram (CTA) by placing digital marks around the orifice of each branch vessel on the CTA (Fig 1). These marks were saved, and an intraoperative noncontrast abdominal CT was then performed before sterile preparation and draping, a process that takes no more than 2 or 3 minutes, which adds little to the overall operating room time.

The Artis zee system acquires (Dyna CT) images by rotating around the patient 200° and obtaining an array of equally spaced 2D x-ray projection images. For
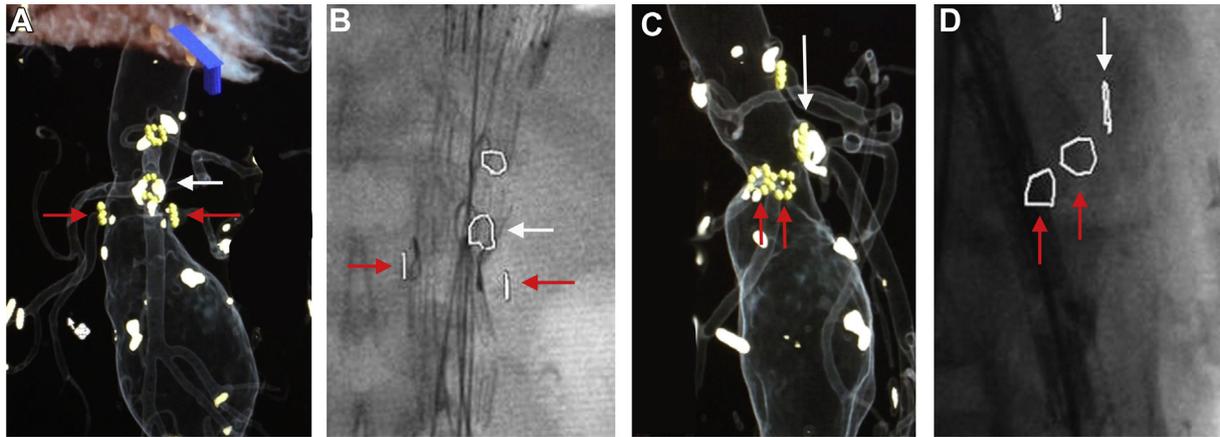
**Fig 1.** This image demonstrates the method of overlay mark production and use. **A,** Marks are placed around the origins of the superior mesenteric artery (*white arrow*) and renal arteries (*red arrows*). **B,** The intraoperative overlay of these marks is shown on live fluoroscopy, and the radiopaque markers on the graft can be seen to closely approximate these overlay marks during deployment. **C** and **D,** Images are shown for the same patient in a lateral projection. Note that a perfectly orthogonal image of the vessel origin can be obtained by aligning the origin marker such that it appears as a line on the overlay, and this can be aligned before fluoroscopy is initiated, minimizing radiation during adjustment of the C-arm.

performance of our overlay imaging with the preoperative CTA, the system initially acquired a noncontrasted CT centered at the visceral segment of the aorta (133 frames over 5 seconds). The images were sent to the Leonardo workstation to create the native mask (bony anatomy and vascular structures) Dyna CT. Dyna CT image data sets were then reconstructed as a 3D image on the Syngo X workplace (Siemens). Next, this intraoperative noncontrasted CT image was fused to the preoperative CTA using bony landmarks.

After sterile preparation, draping, and obtaining arterial access, stiff Lunderquist wires (Cook Medical, Bloomington, Ind) were placed, and IVUS imaging was used to confirm the preoperatively placed marks, which are seen as an overlay image on live fluoroscopy (Fig 1). Next, the vessel origin overlay image was adjusted to correspond to the IVUS image with the stiff wires in place before device delivery. The device was then inserted and deployed using the radiopaque graft markers and the overlay marks displayed on live fluoroscopy. Notably, contrast was not routinely given or required until after each branch vessel was revascularized using a stent graft.

The 3D overlay image was used selectively to confirm the wire path as the target vessel of interest, decreasing the need for DSA during fenestration/branch catheterization. DSA was typically reserved for a completion aortogram or during difficult vessel catheterizations. In patients requiring iliac limbs, IVUS imaging was used to determine the hypogastric location, and contrast injections were typically not used for iliac limb deployment. Similar to FEVAR performed in the other hybrid operating room, contrast was diluted to one-third strength for all hand-injection imaging and to one-half strength for completion DSA. Notably, the power injector was not routinely used until the completion aortogram, and to prevent settling

of contrast, the one-half strength mixed contrast was not loaded until the time of the aortogram.

**Radiation dose calculation.** Radiation exposure is reported as the cumulated air kerma (CAK), recorded as mGy, along with total fluoroscopy time (minutes), both of which are routinely collected in our hybrid operating rooms for each procedure. Kerma is an acronym for "kinetic energy released per unit mass," and provides an international standard for estimating radiation dose. Notably, our Toshiba Infinix VC-i system and the Siemens Artis zee system have similar methods of CAK determination. This method is guided by Food and Drug Administration standards, with the reference location for determination of CAK at 15 cm from the isocenter toward the x-ray source along the beam axis.

**End points and statistics.** Primary end points included radiation dose (CAK), fluoroscopy time, contrast use, and procedure time (defined as time from skin incision/puncture to bandage application). Secondary end points analyzed included total estimated blood loss, length of stay, complications, and 30-day mortality. Complications were defined and tabulated based on reporting standards for endovascular aneurysm repair.[21] Estimated glomerular filtration rate (eGFR) was calculated using the Chronic Kidney Disease Epidemiology Collaboration (CKD-EPI) formula.[23]

Differences in renal function were calculated using the nonparametric Kruskal-Wallis and exact Wilcoxon scores tests. Continuous variables were analyzed using the Student *t*-test or Wilcoxon Mann-Whitney test, and categoric variables were compared with a $\chi^2$ or Fisher exact test, when indicated. All analysis was completed using R 2.15.0 software (The R Foundation for Statistical Computing, Vienna, Austria). A *P* value of <.05 was considered significant.

**Table I.** Demographics and comorbidities for all patients

| Feature[a] | No CT (n = 41) | 3D CT (n = 31) | P value[b] |
|---|---|---|---|
| Age, years | 71 ± 7 | 72 ± 11 | .6 |
| Male sex | 32 (78) | 21 (67) | .5 |
| Body mass index, kg/m$^2$ | 30 ± 6 | 26 ± 4 | .01 |
| Comorbidity | | | |
| Hypertension | 39 (95) | 25 (81) | .06 |
| Dyslipidemia | 23 (56) | 16 (51) | .8 |
| Chronic pulmonary disease | 20 (48) | 11 (35) | .3 |
| Smoking | 18 (43) | 16 (51) | .6 |
| Coronary artery disease | 18 (44) | 12 (39) | .8 |
| Diabetes mellitus | 12 (29) | 8 (25) | .8 |
| Cerebrovascular disease | 10 (14) | 6 (15) | 1 |
| Chronic renal insufficiency[c] | 8 (19) | 7 (22) | .8 |
| Congestive heart failure | 6 (14) | 3 (9) | .7 |
| Arrhythmia | 5 (12) | 3 (9) | 1 |
| End-stage renal disease | 0 | 2 (7) | .2 |

*3D CT*, Three-dimensional fusion computed tomography; *No CT*, no intraoperative computed tomography.
[a]Continuous data are expressed as mean ± standard deviation and categoric data as number (%).
[b]*P* values were determined with *t*-tests, $\chi^2$, or Fisher exact test, when indicated.
[c]Chronic renal insufficiency defined as estimated glomerular filtration rate < 50 mL/min/1.73 m$^2$ and/or Cr > 1.6.

**Table II.** Patient demographics and comorbidities by number of revascularized vessels

| Feature | No CT, No. | 3D CT, No. | P value[a] |
|---|---|---|---|
| Two-vessel FEVAR | 8 | 12 | |
| Hypertension | 7 | 10 | 1 |
| Dyslipidemia | 4 | 8 | .6 |
| Chronic pulmonary disease | 3 | 5 | 1 |
| Smoking | 1 | 1 | .6 |
| Coronary artery disease | 5 | 5 | .6 |
| Diabetes mellitus | 3 | 4 | 1 |
| Cerebrovascular disease | 1 | 1 | 1 |
| Chronic renal insufficiency[b] | 1 | 2 | 1 |
| Congestive heart failure | 1 | 2 | 1 |
| Arrhythmia | 1 | 1 | 1 |
| End-stage renal disease | 0 | 2 | .5 |
| Three-vessel or four-vessel FEVAR | 33 | 19 | |
| Hypertension | 32 | 15 | .05 |
| Dyslipidemia | 19 | 8 | .4 |
| Chronic pulmonary disease | 17 | 6 | .3 |
| Smoking | 17 | 12 | .5 |
| Coronary artery disease | 13 | 7 | 1 |
| Diabetes mellitus | 9 | 4 | .7 |
| Cerebrovascular disease | 5 | 3 | 1 |
| Chronic renal insufficiency[b] | 7 | 5 | .7 |
| Congestive heart failure | 5 | 1 | .4 |
| Arrhythmia | 4 | 2 | 1 |
| End-stage renal disease | 0 | 0 | NA |

*3D CT*, Three-dimensional fusion computed tomography; *FEVAR*, fenestrated endovascular aneurysm repair; *NA*, not applicable; *No CT*, no intraoperative computed tomography.
[a]*P* values were determined with *t*-tests, $\chi^2$, or Fisher exact test when indicated.
[b]Chronic renal insufficiency defined as estimated glomerular filtration rate < 50 mL/min/1.73 m$^2$ and/or Cr > 1.6.

## RESULTS

Between September 2013 and March 2014, 32 patients underwent FEVAR, and 31 of these were performed using 3D fusion CT by a single surgeon (3D-CT group). One FEVAR was performed in the older hybrid operating room due to the emergent nature of the procedure and room availability. In the 12 months prior, 40 patients underwent FEVAR in the non-CT-capable hybrid operating room, and these were combined with the patient described previously, making the total no-CT cohort 41 patients. Demographics, comorbidities, and aneurysm characteristics of all patients are reported in Table I. Notably, the mean body mass index of the two groups is one of the only patient characteristics that was different and was significantly lower in the 3D-CT group (26 ± 4 kg/m$^2$) vs the no-CT group (30 ± 6 kg/m$^2$; *P* = .01). Table II reports demographics and patient characteristics stratified by the number of vessels revascularized.

Radiation exposure (no CT: 5000 ± 280 mGy vs 3D CT: 2200 ± 1300 mGy; *P* < .0001) and fluoroscopy time (no CT, 84 ± 36 minutes vs 3D CT, 55 ± 21 minutes; *P* = .0004) were both significantly lower in the 3D-CT patients (Fig 2, *A* and *B*). In addition, overall contrast use was lower for the 3D-CT patients (34 ± 15 mL) than for no-CT patients (86 ± 25 mL; *P* < .0001). The difference remained significant when divided into two-vessel (no CT [n = 8]: 69 ± 16 vs 3D CT [n = 12]: 26 ± 8; *P* = .0002) and three-vessel and four-vessel (no CT [n = 33]: 90 ± 25 vs 3D CT [n = 19]: 39 ± 17; *P* < .0001) fenestration groups (Fig 2, *C*). Notably, the procedure times were less in the 3D-CT groups, with a much larger effect in the three-vessel and four-vessel patients (Fig 2, *D*). The estimated blood loss was significantly lower estimated in the 3D-CT group (200 ± 180 mL) than in the no-CT group (390 ± 380 mL; *P* < .0001).

**Outcomes.** Several features of the perioperative details that may have affected postoperative outcomes are reported in Table III. Notably, no difference existed in aneurysm size, extent, urgency, or adjunct use. The 30-day
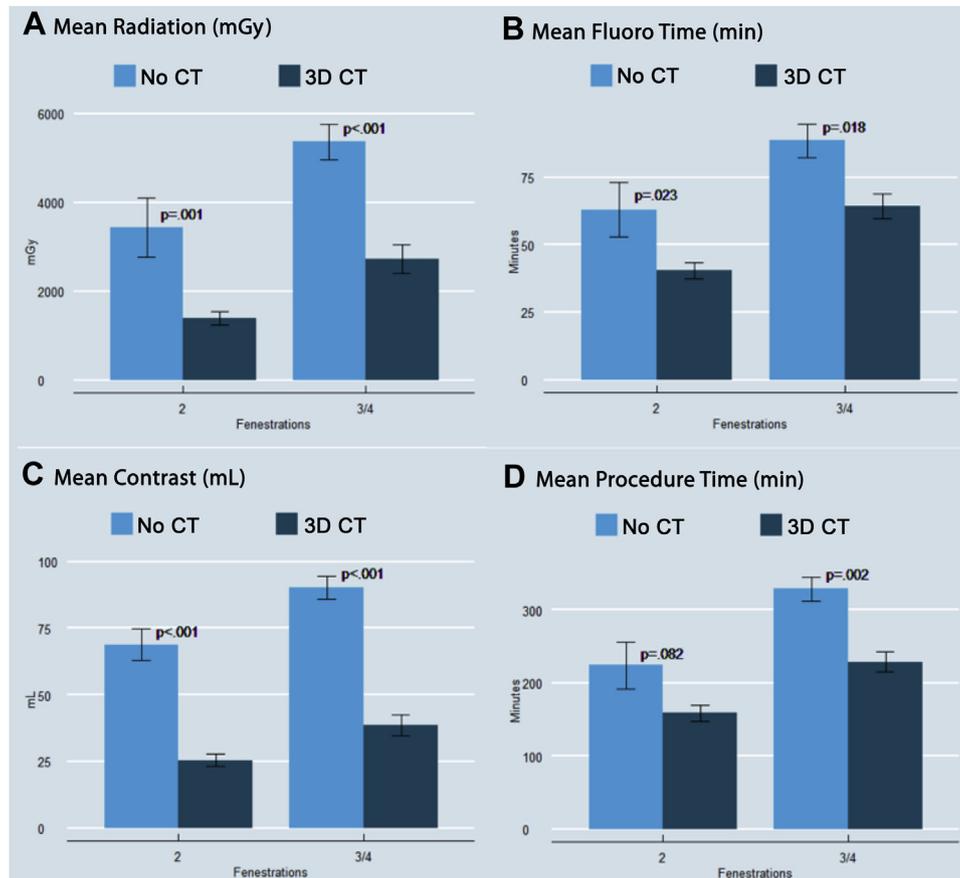
**Fig 2.** This figure demonstrates the reduction in **(A)** radiation exposure, **(B)** fluoroscopy time, **(C)** contrast usage, and **(D)** overall procedural time with use of three-dimensional fusion computed tomography (*3D CT*) technology in fenestrated endovascular aneurysm repair (FEVAR).

mortality between the no-CT and 3D-CT groups was 5% (n = 2) and 3% (n = 1; *P* = 1), respectively. A trend toward a decreased length of stay for the 3D-CT patients (*P* = .07) was also observed. Although no significant differences in the rate of postoperative complications was noted between the no-CT and 3D-CT groups, no spinal cord ischemia events were observed in the 3D-CT group (*P* = .06).

Finally, the rates of endoleak and description of the reinterventions are catalogued in Table IV (any reintervention, 12% for no CT [n = 5] vs 13% for 3D CT [n = 4]; *P* = 1). Fenestration patency (all vessels patent in each group, 34 in no CT vs 27 in 3D CT; *P* = 1) during follow-up did not differ between the two groups. In addition, no significant differences were seen with respect to the eGFR change during follow-up (median [interquartile range] Δ eGFR from preoperative to most recent follow-up: no CT, 0 [−5 to 0] vs 3D CT, 0 [−4 to 1.5]; *P* = .6).

## DISCUSSION

This study demonstrates that intraoperative 3D fusion CT significantly reduces radiation exposure, contrast use, and overall procedural time in FEVAR. Although this study was not powered or designed to detect the effects of this technology on perioperative outcomes, important metrics, including blood loss and length of stay, appeared to be favorably affected. These findings highlight the potential physiologic benefits of implementing innovative imaging techniques in advanced endovascular procedures. In addition, although we were not able to reliably calculate the radiation dosage to the provider who performed these procedures, one may reasonably assume that the substantial reduction in radiation exposure to the patient also translated to decreased exposure to all health care providers participating in these repairs.

A number of factors led to a reduction in radiation exposure and fluoroscopy time in this study. Most importantly, the intraoperative CT and vessel origin overlay facilitate graft deployment and catheterization of the branch vessels, thereby decreasing fluoroscopy time. Additional elements that may have contributed to the observed decrease in radiation dose and fluoroscopy over time include subtle technical aspects regarding the vessel-marking method. Fig 1 demonstrates the markings placed on the vessel origins, which are traced around the orifice

**Table III.** Operative details and postoperative outcomes of all fenestrated endovascular repair (FEVAR) patients

| Feature[a] | No CT (n = 41) | 3D CT (n = 31) | P value[b] |
|---|---|---|---|
| Aneurysm diameter, mm | 67 ± 13 | 65 ± 14 | .3 |
| Suprarenal/TAAA extent | 26 (65) | 21 (72) | .7 |
| Elective | 30 (73) | 26 (84) | |
| Urgent/emergency indication | 11 (27) | 5 (16) | .5 |
| Intraoperative adjunct | 9 (22) | 5 (16) | .8 |
| Estimated blood loss, mL | 390 ± 380 | 200 ± 180 | <.0001 |
| Thirty-day mortality | 2 (5) | 1 (3) | 1 |
| Length of stay, days | 5 (4-11) | 5 (3-8) | .07 |
| Complication | | | |
| Cardiac | 5 (12) | 3 (10) | 1 |
| Pulmonary | 5 (12) | 1 (3) | .2 |
| Renal | 6 (15) | 1 (3) | .2 |
| Bleeding | 3 (7) | 1 (3) | .6 |
| Gastrointestinal | 3 (7) | 1 (3) | .6 |
| Stroke | 1 (2) | 0 | 1 |
| Spinal cord ischemia | 5 (12) | 0 | .06 |

*3D CT,* Three-dimensional fusion computed tomography; *No CT,* no intraoperative computed tomography; *TAAA,* thoracoabdominal aortic aneurysm.
[a]Continuous data are expressed as mean ± standard deviation or median (interquartile range) and categoric data as number (%).
[b]P values were determined with *t*-tests, $\chi^2$, or Fisher exact test when indicated.

immediately at the origin of the branch vessel on the aortic wall, producing a circle on the live fluoroscopy overlay. This circle facilitates precise fluoroscopy usage by allowing the provider to position the C-arm such that a perpendicular view of the vessel will be seen immediately upon initiation of live fluoroscopy. This decreases the overall fluoroscopy time and thus decreases the radiation exposure.

Further, although lateral fluoroscopy is typically required for successful celiac/superior mesenteric artery catheterization and stenting, the C-arm can be positioned such that the desired field of view and vessel orientation are ensured before fluoroscopy is initiated. Also, the fenestrated device markers can be aligned with the vessel origin in the anterior-posterior C-arm position, or in slight obliquity, rather than the full lateral position. Eliminating the need for deep oblique and lateral fluoroscopy in this manner significantly reduces the amount of radiation required.[24] Indeed, reducing the need for prolonged obliquity of the C-arm during FEVAR is tantamount to a reduction of the overall radiation exposure to the patient and operating team alike, and in our opinion, this advantage of 3D fusion CT should be exploited as much as possible.

Lastly, and also very importantly, the need for DSA imaging is greatly decreased with this new technology and is reserved primarily for completion imaging. DSA is used for difficult vessel catheterization at times, but the frequency is diminished substantially with improved imaging and 3D overlay on the live fluoroscopic image, despite the addition of the radiation from the intraoperative CT itself.

We should note that the operator cannot rely entirely on the intraoperative 3D overlay for device deployment due to alterations in branch vessel location with the stiff delivery systems in place. The relationships of the vessels are frequently altered once the stiff wires and delivery system are in the aorta, and the aorta itself may move substantially. The operator thus must be proficient with IVUS imaging and comfortable with manipulating the overlay

to match the IVUS imaging before device deployment. This concept was recently corroborated by Maurel et al[25] in their study demonstrating vessel movement upon introduction of the stiff deployment system during these procedures. Our routine is to perform IVUS imaging with two stiff Lunderquist wires in place and to adjust the overlay to match our IVUS image as closely as possible before device delivery.

With increasing awareness of the possible detrimental health effects of radiation exposure to patients and health care providers, investigators and the developers of imaging products have sought to decrease the radiation required for these procedures.[7,13] Some have suggested that maximum doses of radiation should be used as benchmarks for hospital quality and have shown that education and protocol changes can have a drastic effect on radiation exposure to patient and health care providers.[26,27]

To that end, providing advanced imaging technologies to supplement increasing use of fluoroscopy-based procedures is important, and all of the advanced imaging companies have newer systems with their own respective proprietary technology to reduce radiation exposure. However, the importance of adhering to ALARA (as low as [is] reasonably achievable) principles is equally if not more important. This includes such things as decreasing the time on the fluoroscopy pedal, reducing frame rates, increasing the distance between the provider and the radiation source (especially important during DSA imaging), diligent use of collimation, avoidance of obliquity unless necessary, and the proper use of protective shielding during the procedure. These techniques can also dramatically reduce radiation exposure to patient and health care providers, perhaps as much as any other intervention.[13,28]

In addition, FEVAR has a known association with renal dysfunction and has been reported to have an associated >30% decrement in renal function in 25% to 33% of patients after the procedure.[15,16] This is likely a

**Table IV.** Comparison of endoleak rates and description of reintervention after fenestrated endovascular aneurysm repair (FEVAR) with and without intraoperative three-dimensional (*3D*) fusion computed tomography (*CT*)

| Endoleak type[a] | No CT (n = 32), No. (%) | 3D CT (n = 25), No. (%) | P value[b] |
|---|---|---|---|
| No endoleak | 27 (84) | 19 (76) | |
| Type Ia/b | 0 (0) | 0 (0) | |
| Type II | 3 (9) | 4 (16) | |
| Type III | 2 (6) | 1 (4) | |
| Type IV | 0 (0) | 0 (0) | |
| Indeterminate | 0 (0) | 1 (4) | .4 |

*Description of reinterventions*

No intraoperative CT patients (n = 5)
- Patient 1: Right renal stent extension/relining for stenosis at 11.5 months
- Patient 2: Jejunal arcade pseudoaneurysm embolization at 1.9 months
- Patient 3: Attempted (failed) left renal bridging stent graft for type III endoleak at 0.6 months
- Patient 4: Left renal stent graft and SMA → IMA embolization for type III and type II endoleak at 3.4 months
- Patient 5: Celiac and SMA stent grafts for type III endoleak at 1.3 months

Intraoperative 3D fusion CT patients (n = 4)
- Patient 1: SMA stent for "shuttering" of native SMA by scallop at 0.7 months
- Patient 2: Mesenteric embolization for left colon hemorrhage at 1.3 months
- Patient 3: Celiac stent graft for type III endoleak at 1.3 months
- Patient 4: Left renal artery branch vessel embolization and hematoma evacuation at 0.1 months

*3D CT*, Three-dimensional fusion computed tomography; *No CT*, no intraoperative computed tomography; *IMA*, inferior mesenteric artery; *SMA*, superior mesenteric artery.
[a]Data are based on patients with available contrasted postoperative CT scans.
[b]The *P* value was determined with the Fisher exact test.

multifactorial phenomenon related not only to the patient's underlying medical comorbidities but also to the performance of the operation (atheroemboli and contrast nephropathy), alterations in branch vessel flow due to configuration changes induced by the stents, and to the postoperative contrast-based imaging that is often necessary. All of these factors can be mitigated, and we believe that the initial insult related to the performance of the procedure is an excellent starting point for implementation of renal-protection strategies.

Here we demonstrate that the contrast dose can be reduced by as much as 60% by using advanced imaging techniques and conservative dye use. Of note, we have had a longstanding policy of minimal contrast usage with FEVAR, and in addition to the imaging improvements, we typically use one-third strength Visipaque 320 for hand injection images (both DSA and live fluoroscopy) and one-half strength for completion aortography. The ability to use these decreased concentrations is certainly facilitated by high-quality imaging in both of our hybrid operating rooms.

The limitations of this analysis include that this is a single-surgeon, single-institution experience, which inherently introduces bias into the analysis and may not be applicable to all practices. In addition, the effect of the learning curve on the analysis cannot be fully determined, and there were certainly ongoing improvements in technical efficiency during the course of the study period. Despite this issue, there were no significant differences in contrast, radiation, and dye exposure in the initial 68 patients excluded from the analysis compared with the no-CT control group (data not shown). The lack of staff exposure data is an unfortunate weakness, but inconsistencies in radiation badge usage were such that we felt that a valid analysis would not be possible.

Further, owing to the variability in the complexity of these procedures with respect to access issues, adjunctive procedures, and the variability in visceral anatomy and occlusive disease, we cannot account for the effect of procedural difficulty and the effect on radiation exposure and procedure time. We concluded that an analysis based on revascularized vessels would allow the fairest analysis in terms of difficulty level, and our data suggest that there were no significant differences in the groups before and after the initiation of 3D fusion CT with regard to aneurysm extent or adjunct usage.

Finally, the average body mass index of our 3D-CT patients was lower than the no-CT group, which would certainly bias the total radiation exposure to be lower in the 3D-CT group; however, the fluoroscopy time corroborates the 3D-CT radiation dose data, mitigating this weakness.

## CONCLUSIONS

FEVAR is an evolving technology that offers a reduced physiologic effect of complex aortic repair compared with standard open repair; however, the elevated procedural complexity leads to increased radiation and dye exposure risk. The results of our study demonstrate that use of intraoperative 3D fusion CT imaging during FEVAR decreases radiation exposure, procedure time, and contrast usage.

This technology has promising potential to improve the safety and overall outcomes of these procedures.

## AUTHOR CONTRIBUTIONS

Conception and design: SS, AB
Analysis and interpretation: MM, SS, AB
Data collection: MM, SS
Writing the article: MM, SS, AB
Critical revision of the article: MM, SS, RF, DN, TH, AB
Final approval of the article: MM, SS, RF, DN, TH, AB
Statistical analysis: DN
Obtained funding: Not applicable
Overall responsibility: SS
M. M. and S. S. participated equally and share first authorship.

## REFERENCES

1. Greenberg R, Eagleton M, Mastracci T. Branched endografts for thoracoabdominal aneurysms. J Thorac Cardiovasc Surg 2010;140: S171-8.
2. Haulon S, Greenberg RK. Part two: treatment of type IV thoracoabdominal aneurysms—fenestrated stent-graft repair is now the best option. Eur J Vasc Endovasc Surg 2011;42:4-8.
3. Kristmundsson T, Sonesson B, Dias N, Tornqvist P, Malina M, Resch T. Outcomes of fenestrated endovascular repair of juxtarenal aortic aneurysm. J Vasc Surg 2014;59:115-20.
4. Kirkwood ML, Arbique GM, Guild JB, Timaran C, Chung J, Anderson JA, et al. Surgeon education decreases radiation dose in complex endovascular procedures and improves patient safety. J Vasc Surg 2013;58:715-21.
5. Berrington de Gonzalez A, Mahesh M, Kim KP, Bhargavan M, Lewis R, Mettler F, et al. Projected cancer risks from computed tomographic scans performed in the United States in 2007. Arch Intern Med 2009;169:2071-7.
6. Chen J, Einstein AJ, Fazel R, Krumholz HM, Wang Y, Ross JS, et al. Cumulative exposure to ionizing radiation from diagnostic and therapeutic cardiac imaging procedures: a population-based analysis. J Am Coll Cardiol 2010;56:702-11.
7. Einstein AJ, Henzlova MJ, Rajagopalan S. Estimating risk of cancer associated with radiation exposure from 64-slice computed tomography coronary angiography. JAMA 2007;298:317-23.
8. Fazel R, Krumholz HM, Wang Y, Ross JS, Chen J, Ting HH, et al. Exposure to low-dose ionizing radiation from medical imaging procedures. N Engl J Med 2009;361:849-57.
9. Howells P, Eaton R, Patel AS, Taylor P, Modarai B. Risk of radiation exposure during endovascular aortic repair. Eur J Vasc Endovasc Surg 2012;43:393-7.
10. Kaul P, Medvedev S, Hohmann SF, Douglas PS, Peterson ED, Patel MR. Ionizing radiation exposure to patients admitted with acute myocardial infarction in the United States. Circulation 2010;122: 2160-9.
11. Maurel B, Sobocinski J, Perini P, Guillou M, Midulla M, Azzaoui R, et al. Evaluation of radiation during EVAR performed on a mobile C-arm. Eur J Vasc Endovasc Surg 2012;43:16-21.
12. Miller DL, Hilohi CM, Spelic DC. Patient radiation doses in interventional cardiology in the U.S.: advisory data sets and possible initial values for U.S. reference levels. Med Phys 2012;39:6276-86.
13. Mohapatra A, Greenberg RK, Mastracci TM, Eagleton MJ, Thornsberry B. Radiation exposure to operating room personnel and patients during endovascular procedures. J Vasc Surg 2013;58:702-9.
14. Noor M, Shekhdar J, Banner NR. Radiation exposure after heart transplantation: trends and significance. J Heart Lung Transplant 2011;30:309-14.
15. Haddad F, Greenberg RK, Walker E, Nally J, O'Neill S, Kolin G, et al. Fenestrated endovascular grafting: the renal side of the story. J Vasc Surg 2005;41:181-90.
16. Verhoeven EL, Vourliotakis G, Bos WT, Tielliu IF, Zeebregts CJ, Prins TR, et al. Fenestrated stent grafting for short-necked and juxtarenal abdominal aortic aneurysm: an 8-year single-centre experience. Eur J Vasc Endovasc Surg 2010;39:529-36.
17. Varu VN, Greenberg JI, Lee JT. Improved efficiency and safety for EVAR with utilization of a hybrid room. Eur J Vasc Endovasc Surg 2013;46:675-9.
18. von Segesser LK, Marty B, Ruchat P, Bogen M, Gallino A. Routine use of intravascular ultrasound for endovascular aneurysm repair: angiography is not necessary. Eur J Vasc Endovasc Surg 2002;23:537-42.
19. Scali ST, Waterman A, Feezor RJ, Martin TD, Hess PJ Jr, Huber TS, et al. Treatment of acute visceral aortic pathology with fenestrated/branched endovascular repair in high-surgical-risk patients. J Vasc Surg 2013;58:56-65.e51.
20. Chaikof EL, Blankensteijn JD, Harris PL, White GH, Zarins CK, Bernhard VM, et al. Reporting standards for endovascular aortic aneurysm repair. J Vasc Surg 2002;35:1048-60.
21. Chaikof EL, Fillinger MF, Matsumura JS, Rutherford RB, White GH, Blankensteijn JD, et al. Identifying and grading factors that modify the outcome of endovascular aortic aneurysm repair. J Vasc Surg 2002;35:1061-6.
22. De Sart K, Scali ST, Feezor RJ, Hong M, Hess PJ Jr, Beaver TM, et al. Fate of patients with spinal cord ischemia complicating thoracic endovascular aortic repair. J Vasc Surg 2013;58:635-42.e632.
23. Levey AS, Stevens LA, Schmid CH, Zhang YL, Castro AF 3rd, Feldman HI, et al. A new equation to estimate glomerular filtration rate. Ann Intern Med 2009;150:604-12.
24. Miller DL, Balter S, Cole PE, Lu HT, Berenstein A, Albert R, et al. Radiation doses in interventional radiology procedures: The RAD-IR study: part II: skin dose. J Vasc Interv Radiol 2003;14:977-90.
25. Maurel B, Hertault A, Sobocinski J, Le Roux M, Martin Gonzalez T, Azzaoui R, et al. Techniques to reduce radiation and contrast volume during EVAR. J Cardiovasc Surg (Torino) 2014;55:123-31.
26. Duncan JR, Street M, Strother M, Picus D. Optimizing radiation use during fluoroscopic procedures: a quality and safety improvement project. J Am Coll Radiol 2013;10:847-53.
27. Duran A, Hian SK, Miller DL, Le Heron J, Padovani R, Vano E. A summary of recommendations for occupational radiation protection in interventional cardiology. Catheter Cardiovasc Interv 2013;81: 562-7.
28. Wagner LK, Archer BR, Cohen AM. Management of patient skin dose in fluoroscopically guided interventional procedures. J Vasc Interv Radiol 2000;11:25-33.